

Conference of Fundamental Research and Particle Physics, 18-20 February 2015, Moscow,
Russian Federation

Gamma-telescopes Fermi/LAT and GAMMA-400 trigger systems event recognizing methods comparison

I.V. Arkhangelskaja*, A.E. Murchenko, E.N. Chasovikov, A.I. Arkhangelskiy, M.D. Kheyimits

National Research Nuclear University MEPhI (Moscow Engineering Physics Institute), Kashirskoe Shosse 31, Moscow, 115409, Russia

Abstract

Usually instruments for high-energy γ -quanta registration consists of converter (where γ -quanta produced pairs) and calorimeter for particles energy measurements surrounded by anticoincidence shield used to events identification (whether incident particle was charged or neutral). The influence of pair formation by γ -quanta in shield and the backplash (moved in the opposite direction particles created due high energy γ -rays interact with calorimeter) should be taken into account. It leads to decrease both effective area and registration efficiency at $E > 10$ GeV. In the presented article the event recognizing methods used in Fermi/LAT trigger system is considered in comparison with the ones applied in counting and triggers signals formation system of gamma-telescope GAMMA-400.

The GAMMA-400 (Gamma Astronomical Multifunctional Modular Apparatus) will be the new high-apogee space γ -observatory. The GAMMA-400 consist of converter-tracker based on silicon-strip coordinate detectors interleaved with tungsten foils, imaging calorimeter make of 2 layers of double (x, y) silicon strip coordinate detectors interleaved with planes of CsI(Tl) crystals and the electromagnetic calorimeter CC2 consists only of CsI(Tl) crystals. Several plastics detections systems used as anticoincidence shield, for particles energy and moving direction estimations. The main differences of GAMMA-400 constructions from Fermi/LAT one are using the time-of-flight system with base of 50 cm and double layer structure of plastic detectors provides more effective particles direction definition and backplash rejection. Also two calorimeters in GAMMA-400 composed the total absorption spectrometer with total thickness $\sim 25 X_0$ or $\sim 1.2 \lambda_0$ for vertical incident particles registration and $54 X_0$ or $2.5 \lambda_0$ for laterally incident ones (where λ_0 is nuclear interaction length). It provides energy resolution 1-2% for 10 GeV– 3.0×10^3 GeV events while the Fermi/LAT energy resolution does not reach such a value because of its calorimeter thickness is only $\sim 10 X_0$ and energy of registered particles is defined by shower profile analysis. Less than 3% photons will be wrongly recognized as electrons or protons in double-layer ACTop taking into account both temporal and amplitude trigger marker analysis methods during onboard processing in the counting and triggers signals formation system of GAMMA-400. The proton rejection factor will be $\sim 10^{-5}$.

The Fermi/LAT based on a 4×4 array of identical towers each contains a tracker, calorimeter and data acquisition module. Each tracker consists of 18 x-y silicon-strip layers. The calorimeter in each tower made of eight layers in a hodoscopic arrangement for measure the three-dimensional profiles of showers permits corrections for energy leakage and enhances the capability to discriminate hadronic cosmic rays. The each layer consists of 12 CsI(Tl) based bars. The segmented anticoincidence shield covers the array of towers. Unfortunately, several types of biases lead to systematic effects caused high values of relative systematic uncertainties of the exposure, the number of signal events, the induced fractional signal and so on. For example non confirmed announcement of ~ 133 GeV line detection and lost sources in different Fermi catalogues (1FGL, 2FGL, 3FGL) – just well seen in 2FGL Cygnus X-3 (J2032.1+4049) does not appear in 3FGL. It allows to conclude sufficient biases in LAT characteristics obtained methods and event recognized algorithms. Now Fermi/LAT operates during ~ 7 years but effective

* Corresponding author. Tel.: +7-916-668-5051.
E-mail address: irene.belousova@usa.net

caveats methods continuously to be proposed. Respectively, continuation of measurements with use of other telescopes is necessary, and realization of GAMMA-400 will allow improving the results.

© 2015 The Authors. Published by Elsevier B.V. This is an open access article under the CC BY-NC-ND license

(<http://creativecommons.org/licenses/by-nc-nd/4.0/>).

Peer-review under responsibility of the National Research Nuclear University MEPhI (Moscow Engineering Physics Institute)

Keywords: GAMMA-400; Fermi/LAT; backslash rejection; trigger system

1. Introduction

Now the most interest results of astrophysical gamma-ray sources, diffuse gamma-emission and cosmic rays investigation were obtained using the Fermi/LAT data. Fermi/LAT is the satellite astrophysics observatory launched in June, 2008 into a circular orbit round the Earth (height of 565 km), intended to registration of space γ -ray emission in the energy range from ~ 20 MeV to >300 GeV. It was designed for studying of charged particles acceleration mechanisms in the active galaxies nuclei, pulsars and supernovae; the unidentified EGRET sources nature definition; detailed investigation of diffuse γ -ray emission (galactic and extragalactic), high-energy γ -ray bursts; research of a dark matter and Metagalaxy [1].

GAMMA-400 (Gamma Astronomical Multifunctional Modular Apparatus) the high-apogee space astrophysics observatory is being constructed at present time. It is designed for registration of galactic and extragalactic γ -rays and charged particles fluxes [2, 3]. This observatory consist of gamma-telescope GAMMA-400, two star sensors for determining the GAMMA-400 axes with accuracy of approximately 5", two magnetometers and KONUS-FG gamma-ray burst monitor (4 position sensitive and 2 spectrometric detectors). The GAMMA-400 main scientific tasks are: receiving energy spectra of galactic and extragalactic diffuse and isotropic γ -rays emission, search of anomalies in γ -ray spectra; registration of electrons and positrons with energy higher than 1 GeV and obtaining its energy spectra; investigation of known and newly observed galactic and extragalactic discrete high energy γ -rays sources; identification of discrete gamma objects with known sources of emission in other energy ranges; measurement of light nuclei galactic isotopes fluxes; registration of high-energy γ -rays and fluxes of electrons and positrons from solar flares. In addition, it allows search and study of γ -ray bursts in the ranges of 10 keV – 15 MeV due to KONUS-FG instrument and more than 0.1 GeV due to GAMMA-400 telescope.

2. Gamma-telescopes structure

There are three types of gamma-quanta interaction with medium: photo interaction, Compton interaction and an electron-positron pair's formation. The last type of interaction is most possible for high energy quanta and defines the structure of instruments for high energy gammas registration. Usually it consists of converter-tracker where the pair formation occurs and calorimeter for energy measurement. Both instrument parts are surrounded by anticoincidence shield. Incident particles primarily pass through the anticoincidence shield, which is sensitive to charged particles, then through thin layers of high-Z material called conversion foils. Photon conversions are facilitated in the field of a heavy nucleus. After a conversion, the trajectories of the resulting electron and positron are measured by particle tracking detectors, and their energies are then measured by a calorimeter.

As it was mentioned above, the primary interaction of photons with matter in the Fermi/LAT and gamma-telescope GAMMA-400 energy range is pair production. For its registration, tungsten plates are applied in the converter-tracker that also contains double (x, y) silicon-strip coordinate detectors. As tungsten is a heavy element ($Z=74$), and cross section of pair formation $\sigma_{e^+e^-} \sim Z_N^2$ it means that γ -quantum, passing through a tracker, will interact with plates only in such a way, and other processes can be neglected. Thus, in the converter-tracker γ -quanta are converted in an e^+e^- pair then registered in other detectors. This process forms the basis for the underlying measurement principle by providing a unique signature for gamma rays, which distinguishes them from charged cosmic rays whose flux is as much as 10^5 times larger, and allowing a determination of the incident photon directions via the reconstruction of the trajectories of the resulting electron-positron pairs.

Fig. 1a presents the scheme of gamma-telescope Fermi/LAT [1, 6-7]. The baseline LAT is modular, consisting of a 4×4 array of identical towers. Each 40×40 cm² tower comprises a tracker, calorimeter and data acquisition module. The tracking detector consists of 18 x-y layers of silicon-strip detectors. It is well-matched to the requirements of high detection efficiency ($>99\%$), excellent position resolution (<60 μ m in this design), large signal: noise ($>20:1$), negligible crosstalk, and ease of trigger and readout with no consumables. The calorimeter in each tower consists of eight layers of 12 CsI(Tl) bars in a hodoscopic arrangement, read out by photodiodes, for a total

thickness of 10 radiation lengths. Owing to the hodoscopic configuration, the calorimeter can measure the three-dimensional profiles of showers permits corrections for energy leakage and enhances the capability to discriminate hadronic cosmic rays. The anticoincidence shield covers the array of towers, employs segmented tiles of scintillator, read out by wavelength-shifting fibers and miniature phototubes.

The LAT is self triggered; events that cause detector hits in three planes automatically trigger readouts of each tower and the anticoincidence system. The characteristic γ -ray signature in the LAT is therefore no signal in the anticoincidence shield, more than one track starting from the same location within the volume of the tracker, and an electromagnetic shower in the calorimeter. Efficient rejection of the charged particle background, which is thousands of times more intense than the celestial γ -ray emission, is essential for Fermi to function. The raw trigger rate in orbit is average a few kHz and the rate of celestial γ -rays a few Hz. The anticoincidence system is only the first line of defense in identifying cosmic rays that trigger the telescope. Other discriminators (according to simulations data) against charged particles have been developed to further reduce the background level. Some of the discriminators are applied onboard to reduce the trigger rate to the ~ 30 Hz rate that can be stored and downlinked.

Fig. 1c presents the γ -telescope GAMMA-400 physical scheme [2, 3], and the backslash effect (see below). **AC** - anticoincidence system (one top and four lateral detectors); **C** - converter-tracker; **S1, S2** - scintillation detectors of time-of-flight system (TOF); **S3, S4** - scintillation detectors of calorimeter (SDC); **CC1** - position-sensitive calorimeter; **CC2** - electromagnetic calorimeter; **LD** - four lateral detectors of the calorimeter (4); **ND** - neutron detector.

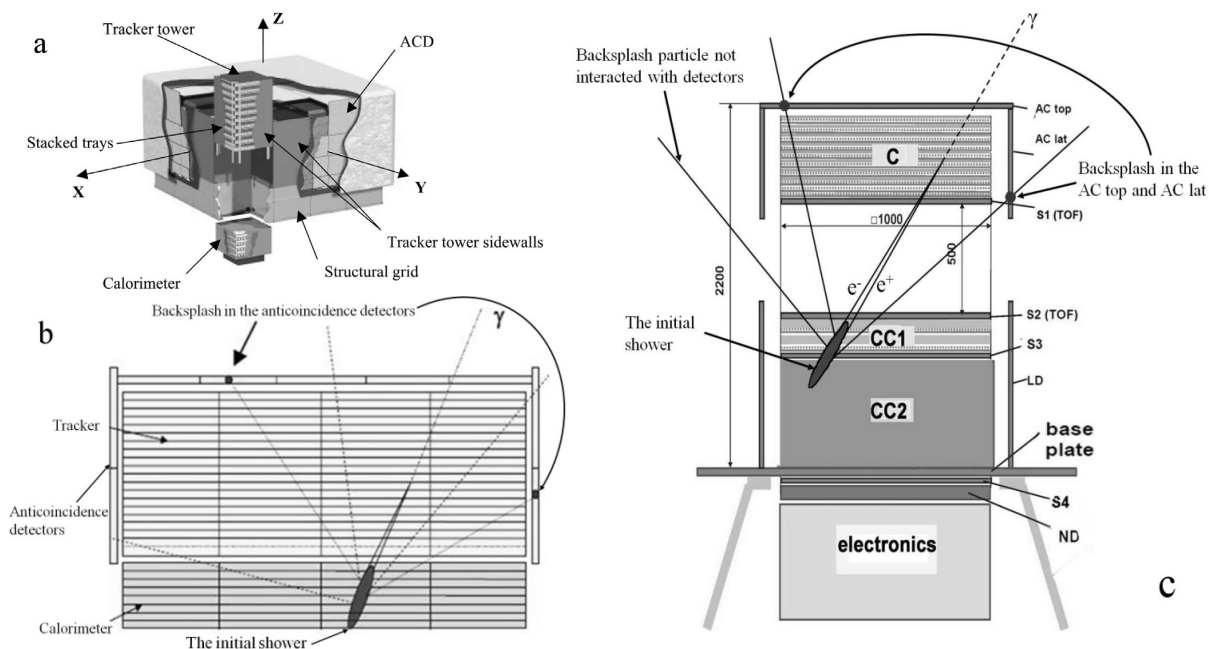


Fig. 1. Backslash illustrations: (a) scheme of the gamma-telescope Fermi/LAT [8] (the anticoincidence detector covered by the micrometeoroid shield and thermal blanket, and the tower module with an 18 layer tracker on top of a hodoscopic calorimeter are shown), (b) backslash effect in the Fermi/LAT, (c) the gamma-telescope GAMMA-400 physical scheme and backslash appearance.

Converter-tracker consists of 13 layers of silicon-strip coordinate detectors (each is double sheets (x, y) with pitch of 0.08 mm) [4]. The first three and final one layers are without conversion foils. Each of the middle nine layers precedes with tungsten foils. The first foil thickness is $0.2 X_0$ and other ones are $0.1 X_0$ (where X_0 is radiation length). Calorimeter consists of two CsI(Tl) based differing parts (CC1 and CC2). CC1 contains two strips layers following of two scintillation detectors ones. AC, S1 - S4 and LD are double layer polyvinyltoluene BC-408 based scintillation detectors. Time-of-flight system defines the incident particle direction. The counting and triggers signals formation system [5] started the data acquisition and provides particle identification due to the individual anticoincidence system detectors signals analysis taking in to account specially designed for GAMMA-400 algorithms of backslash rejection by means of time-of-flight and segmentation methods - see Fig.2 (backscattering particles created when high energy γ -rays interact with the calorimeter's matter and move in the opposite direction). Three apertures allow particles detection from upper and lateral

directions. The main aperture allows the best angular (all strip layers information analysis) and energy (energy deposition in the all detectors studying) resolution. Gamma-telescope GAMMA-400 is able to detect gamma-rays, electrons (positrons) in the energy range from 0.1 GeV– 3.0×10^3 GeV and light nuclei in the main aperture. It is optimized for the particles with energy $\sim 1.0 \times 10^2$ GeV with following parameters [3, 4]: the angular resolution $\sim 0.01^\circ$, the energy resolution $\sim 1\%$, and the proton rejection factor $\sim 5 \times 10^5$. The main aperture also allows investigating high-energy light nuclei fluxes characteristics. The effective area of GAMMA-400 in this aperture is $\sim 4000 \text{ cm}^2$ at $E_\gamma > 1 \text{ GeV}$ [4].

The main difference between Fermi construction is the presense of TOF system and double layer in each plastic detectors provides more effective particles direction definition and backplash rejection. Also the two calorimeters in GAMMA-400 composed the total absorbtion spectrometer [2 – 4] due to its total thickness ($\sim 25 X_0$ or $\sim 1.2 \lambda_0$ for vertical incident particles registration and $54 X_0$ or $2.5 \lambda_0$ for laterally incident ones (where λ_0 is nuclear interaction length)). It provides energy resolution 1-2% for $10\text{--}3.0 \times 10^3$ GeV events, while the Fermi/LAT energy resolution does not reach such a value because of its calorimeter is only $\sim 10 X_0$ thick.

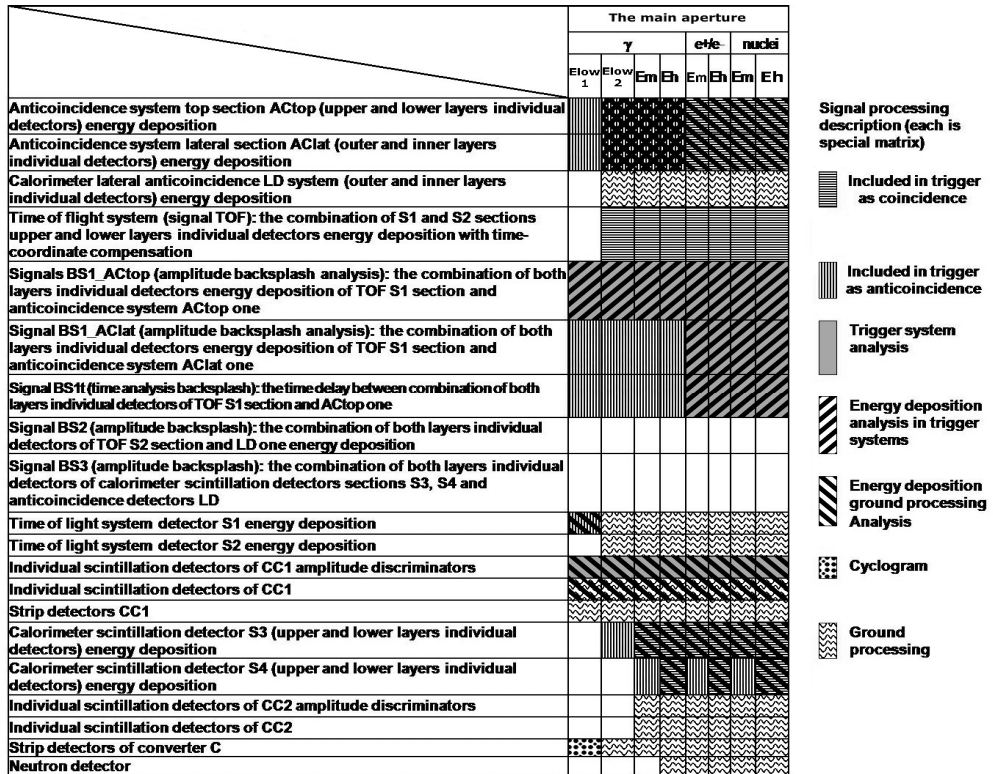


Fig. 2. The GAMMA-400 counting and triggers signals formation system simplified scheme for the main aperture.

3. Backsplash rejection and event recognizing

As result of backplash effect (see Fig. 1b), the γ -quantum could be identified as charged particle. Gamma-quanta in the GAMMA-400 main aperture are identified with absence of impinged particles corresponding signal in the AC taking into account backplash influence rejection based on time-of-flight (because of it delays from time of incident particles direct interaction in ACTop) and segmentation methods [2, 3, 5]. Electrons (positrons) and nuclei recognized by signals corresponding to energy deposition in the individual detectors of AC, S1, S2, S3 and fast signals from CC1 individual detectors discriminators (for simplified algorithm illustration see Fig. 2). The time delay of backplash signal depends on the distance between ACTop and other elements in which backplash produced (conversion foils, CsI(Tl) crystals and so on) exceeds TOF system vertical size. In the gamma-telescope Fermi/LAT (which has single-layer system of anticoincidence) only segmentation of anticoincidence shield is used for backplash rejection.

Taking into account backslash rejection algorithms [5], the energy deposition distributions in ACtop upper and lower layers for gammas with initial energy 3 GeV are presented at Fig. 3a. Only 2.8% of photons will be wrongly recognized (208 particles from 7500) as electrons or protons in double-layer ACtop taking into account both temporal and amplitude trigger marker analysis methods during onboard processing in the counting and triggers signals formation system. The thresholds were defined for relativistic protons and electrons - see Fig. 3b. The proton rejection factor will be $\sim 10^{-5}$.

As example the γ -quanta interaction with the GAMMA-400 anticoincidence detectors substance modeling results for randomly selected of sequence of 5 particles are presented in the Table 1 (totally 10^5 events were simulated). The gammas were impinged via the detector #6 in the top layer of ACtop and the one #19 in the lower layer (strictly vertical passing). The obtained data analysis shows that in single-layer anticoincidence system consisting of parallel detectors about 5% of γ -quanta may give energy deposition due to pair production.

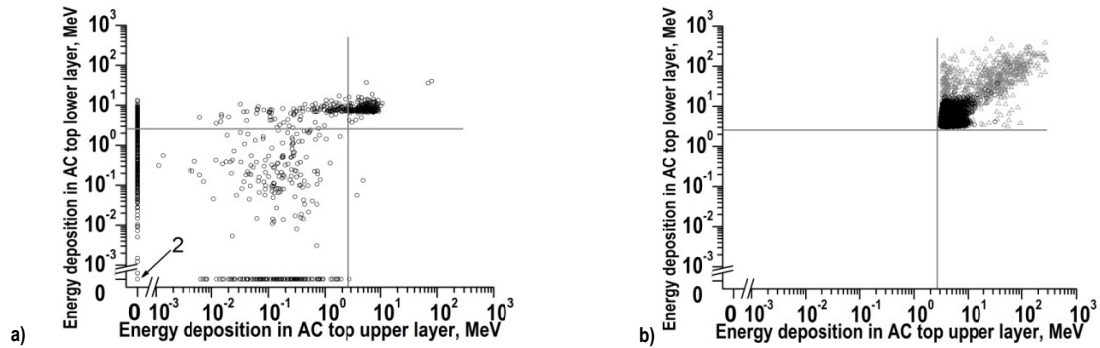


Fig. 3. Energy deposition in double layers ACtop: a) for 3 GeV gamma-quanta with backslash subtraction using temporal analysis (area marked (2) contains $\sim 70\%$ of events with energy deposition less than 1 keV in both ACtop layers); b) for relativistic protons (grey) and electrons (black) used for thresholds definition.

Table 1. The results of modeling γ -quanta interaction with ACtop detectors' substance. Energy release from direct γ -quantum interaction marked in bold, from backslash in italic. In the detectors aren't specified in the table, energy release isn't registered.

| # of particle | | Energy deposition, MeV | | | | | | | | | |
|---------------|-------|------------------------|----------------|----------------|----------------|----|---|----------------|----------------|----------------|----------------|
| | | 67 | | 68 | | 69 | | 70 | | 71 | |
| # of detector | | | | | | | | | | | |
| AC_0 | AC_10 | <i>0.00066</i> | <i>0.11820</i> | <i>0.00067</i> | <i>0.01860</i> | 0 | 0 | 0 | 0 | 0 | 0 |
| AC_1 | AC_11 | 0 | 0 | 0 | 0 | 0 | 0 | 0 | 0 | 0 | <i>0.21673</i> |
| AC_5 | AC_15 | 0 | 0 | 0 | 0 | 0 | 0 | 0 | 0 | <i>0.44438</i> | 0 |
| AC_6 | AC_16 | 0 | 0 | 0 | 0 | 0 | 0 | 0.37155 | 0 | 0 | 0 |
| AC_7 | AC_27 | 0 | 0 | 0 | 0 | 0 | 0 | 0 | <i>0.04634</i> | 0 | 0 |
| AC_9 | AC_20 | <i>0.37288</i> | 0 | 0 | 0 | 0 | 0 | 0 | 0 | 0 | 0 |

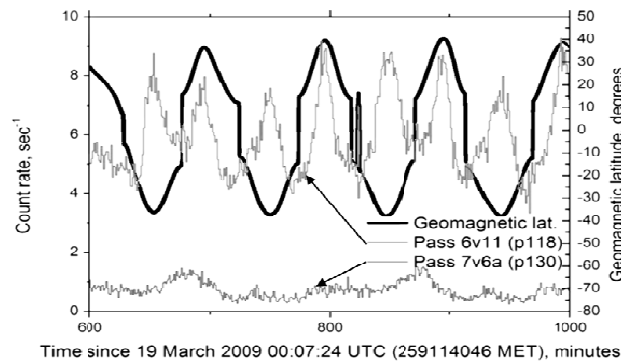


Fig. 4. Temporal profile of the background events count rate identified in experiment of Fermi/LAT as γ -quanta. The thick line shows variation of geomagnetic latitude, thin lines – events count rate (adopted from [7]).

Table 2. The description of Onboard Filter vetoes [1, 7].

| | |
|--------------------|---|
| Veto 30 | Designed to distinguish between background events that cause an ACD tile hit and γ -rays that would otherwise self-veto. Veto 30 is based on assumption that backplash from the CAL it is not likely for a low energy event. It looks to see if there are any events without a CAL LO trigger that have one or more hit ACD filter tiles. In this case veto 30 eliminates the event. |
| Veto 29 | Eliminates events that have a CAL LO trigger, but not a CAL HI, and still show evidence of backplash. The backplash evidence is either 4 or more ACD tiles over threshold (any tiles), or any 3 hit ACD tiles distributed such that one of the tiles is not touching one of the other two on the side or a corner. In Fig. 5 this condition is labeled as “AFC splash()” The AFC splash() condition is present because it might be possible for a γ -quantum to convert to an e^+e^- pair that could then pass out the side of the LAT (depending on the trajectory). This is looking for evidence of backplash, so it looks for tiles that are not clustered. Veto 29 only eliminates lower energy events (without a CAL HI), because eliminating higher-energy events with filter tile hits introduces the danger of γ -ray rejection. |
| Veto 28 and 27 | Veto 28, like veto 30, compares the level of activity in the ACD to that in the CAL. Specifically, it looks to see if there is less than 10 MeV of uncorrected energy in the CAL (when transmitted to the ground, the CAL energy deposit is corrected) and requires that the ACD be completely quiet, or the event will be vetoed. If the ACD has any hits at all, and there is less than 10 MeV in the CAL, it is most likely that the reason for the hit was a cosmic ray. If the energy is more than 10 MeV, but less than 350 MeV, the Filter allows the bottom two rows of the ACD to have tile hits, but the upper ACD filter tiles must have no hits. If there is a low energy event that coincides with ACD hits in the filter tiles, it is most likely because of a cosmic ray. This condition will cause veto 27 to be set. |
| Veto 26 | Uses two types of backplash detection. If the energy in the CAL is less than 40 GeV, but 3 tiles are hit, veto 26 checks the pattern of hits in the ACD. The premise is that the conversion of a γ -quantum could produce secondary particles that pass out the side of the ACD, causing tile hits. Veto 26 checks for tile clustering; if clustering is not found, the event is rejected as background. |
| Veto 21 | Veto 21 (evaluates what is called a Z-bottom veto) designed to remove the events caused by upward-going cosmic rays interacted in the CAL and create upward-going gammas. The Z-bottom veto rejects an event if the event has at least 10 MeV in the CAL, but doesn't show evidence that a particle track is pointing at the CAL (strip hits in any of the 4 of 6 planes of silicon adjacent to the CAL). If 4 planes are hit, and there is greater than 10 MeV, the event is not vetoed. |
| Veto 25 and 24 | The modular design of the LAT allows each tower to self-trigger when there is a 3-in-a-row (when 6 consecutive planes of silicon, or 3 X-Y pairs have hits, a tracker trigger is initiated). Some events might have tracks that do not cause a hit in one of a series of silicon planes. The algorithm first builds a list of those towers that have a 4/4 coincidence (minimum of 4 hit planes out of 4 consecutive silicon planes). Once those towers are identified, vetoes 24 and 25 look within them for either a 7/8 coincidence or a 6/6 coincidence. Once towers with 6/6 and 7/8 coincidences are identified, the algorithm looks for hit ACD tiles that are adjacent to those towers. Veto 25 looks above a “triggered” tower to see if any of the 4 tiles above that tower (that shadow it) are over veto threshold. If so, and if the 6/6 or 7/8 began in the top 3 layers, the veto is activated. The layer condition is present to help ensure a link between the tower trigger and the ACD hit. Veto 24 looks to the side of an edge or corner tower to see if one of the ACD tiles in the upper two rows of the adjacent side face (or faces) is hit. If so, and if the beginning of the 6/6 or 7/8 is at the same height or below the tile, the veto is activated. This layer-height condition is present to guard against the rejection of a γ -ray whose products exit out the LAT side as they travel downwards. If a tower is shadowed by both a side tile and a front face tile, only veto 25 is set for the top face veto, and it is not necessary to look at veto 24 also. These vetoes are present because a triggered tower that is adjacent to a hit ACD tile may be a sign of a cosmic ray that passed through the tile and triggered the tower. |
| Veto 23 and 22 | Veto 23 and 22 deal entirely with energy distributions in the CAL when the event deposits less than 300 MeV. Veto 23 requires that the energy in the layer next to the tracker be 1% to 90% of the total energy deposit in the CAL, because downward-going low energy gammas should deposit a large fraction of their energy in the top layer. If the energy in this layer is less than 1% of the total, veto 23 is set. If the energy in the layer is greater than 90% of the total energy, veto 22 is set. Cosmic rays or gammas, that don't pass through the tracker first may have energy distributions in the CAL that are inconsistent with these ratio checks, and they will be vetoed. |
| Veto 17 | Veto 17 asks if there is any possibility of reconstructing a track. It asks if there are any locations in a tower where there are at least 4 planes of silicon hit in a row. If so, Onboard Filter decides that processing may continue, because this is some indication that the more sophisticated ground reconstruction might be able to find a track. However, if the 4 planes condition is not met, the event is rejected, because many events with few plane hits are low energy background events. |
| Veto 20, 19 and 18 | If an ACD tile is hit, and there is a track pointing to it, the reason was very likely a cosmic ray. Veto 20 checks to see if a track points to a tile in the front of the ACD, while veto 19 checks the upper two rows of the side faces, and veto 18 checks the lower two rows of the side faces. If a hit tile is below the highest tracker hit, the event is not eliminated, because the tile hit could have been caused by a gamma converting in the tracker and its secondary particles passing out the side as they travel downward. Veto 19 is activated if the ACD tile is in the top two rows, and veto 18 is activated if the tile is in the next two rows down. |
| Veto 16 and 15 | Veto 16 asks whether the projections found earlier pass through the gap between the ACD and the top of the CAL. This region is known as the skirt. If an event makes it through the skirt cut, Onboard Filter moves on to the final vetoes. First, the number of projections found earlier is checked. If there was only one projection, veto 17 would be set (this is its second opportunity to get set). If only two projections were found, and the CAL energy is less than 350 MeV, veto 15 is activated. This is because lower energy γ -rays are expected to produce two resolvable tracks, because the separation angle between the resulting e^+e^- pair is large. At least three projections are necessary in order to create two 3-D tracks, so the absence if this signature indicates that the event may have been background. |

In addition, about 60% of energy deposition owing to the backplash and therefore neutral particles may incorrectly recognize as charged ones [4]. Fig. 4 illustrated the similar effect for Fermi/LAT with one layer anticoincidence shield segmented for pieces with lower size [6] than GAMMA-400 individual detectors of ACDtop. It shows the correlations between temporal profile of identified as γ -quanta with $E > 20$ MeV background events count rate in 6.7 hours on 19.03.2009 and dependence of the Fermi/LAT γ -telescope position in the Earth magnetic field on time. Such correlation is possible only for charged particles registration (neutral γ -quanta do not interact with magnetic field). It's evident of inefficient onboard particles identification due to anticoincidence and trigger systems (some protons are registered as γ -quanta). Of course, subsequent ground data processing using special algorithms (so-called passes) reduced the most part of charged particles but geomagnetic modulation presents up to shown by lower curve at Fig. 4 results of using Pass 7v6a [9].

The Fermi/LAT event filtering code consisted of 16 different cuts or reasons to veto an event. Vetoes that used a minimum of processing power and were also likely to occur at a high rate were placed before those that were predicted to be less frequent [7]. When onboard filter determines whether an event should be vetoed, it notes the reason for the veto in a 32-bit summary word. The first 15 bits (numbered 0 to 14) are status bits that can be used for debugging, and the next 16 bits are used to describe which vetoes are active for that event. The remaining summary bit is set if the event is vetoed for any reason. Because of the bit placement, the vetoes are numbered from 15 to 30, and because of the order, in which the vetoes occur within the code, the first veto encountered in the algorithm is veto 30 and the last one is veto 15. The only two deviations from the veto ordering scheme are when vetoes 21 and 17 appear before they would otherwise be expected. Describing of the onboard filter veto is shown in Table 2 [1, 7]. Fig. 5 shows the revised logic of the onboard filter [7].

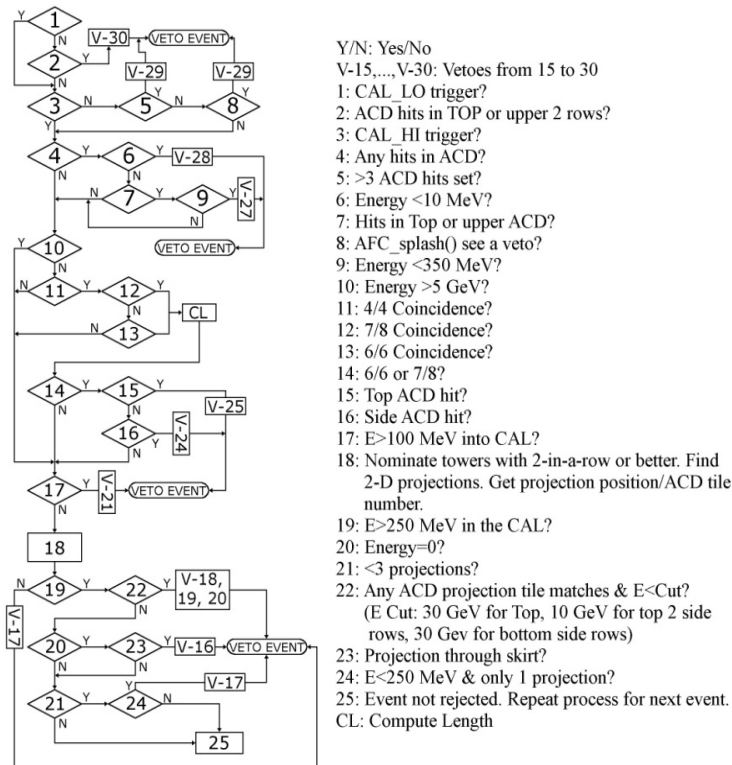


Fig. 5. Revised onboard filter logic. Adopted from [7].

Several caveats methods were presented for the photon dataset biases in experiment Fermi/LAT (for example, Pass 7v6a [9] and its updated version P7REP [10]). Unfortunately, some limitations occur during these methods applications. For example, the tool for small transient sources analysis ("P7REP_TRANSIENT") was implemented only for short transient events (for example, gamma-ray bursts) lasted less than 200 s otherwise the large non-photon backgrounds events amount strongly influence to the data analysis quality [9, 10]. Also recommended for all point sources "P7REP_SOURCE" method may result in spurious spectral features during integrating over large regions of the sky and "P7REP_CLEAN" algorithm advised to be used for diffuse emission studies at high energies [10] shows biases too. The typical example of such biases appearance is announcement of the feature around 133 GeV detection at 3.2σ level [11]. Such patterns are very important for dark matter searches and this feature widely discussed during several years following new hypothesis formulation (see, for example, [12]). But the investigation of systematic effects due to caveats method P7REP [10] shown high values of relative uncertainties of the exposure, the number of signal events, the induced fractional signal and so on [13]. For example, the number of signal events uncertainty could be (+7/-12)% for energy range leads to underestimate the signal by 7% at $E_\gamma \sim 70$ GeV, mistaken interpretation of a true 5σ signal to be only 4.4σ or increased a 3σ fluctuation to be 3.2σ [13]. Thus, the fit significance of ~ 133 GeV feature detection reduces to only 1.5σ

and it being much narrower than the Fermi/LAT energy resolution [13] and only authenticate the necessity to investigate this energy band by means of instrument with the better energy resolution than Fermi/LAT. However, the authors of [13] hoped Pass 8 improved energy resolution, while the local significance of this feature also decreases down to 0.72σ [14]. The authors of [14] also will expected “the sensitivity of future line searches with the LAT will increase with continued exposure”, but now is the 7th year of Fermi/LAT operation and it is anomaly long period for waited patiently database reprocessing.

Three catalogs of sources 1FGL, 2FGL and 3FGL were published by the results of Fermi/LAT observations – see [8] and references therein. However 346 sources from 1FGL weren't identified in 2FGL and 300 ones from 2FGL weren't recognized in 3FGL, and some sources continue identified in other energy ranges in the SIMBAD and NED catalogs. It's galaxies of NGC 1218, NGC 6241, NGC 6541, 5 pulsars, etc. Moreover, Cygnus X-3 (2FGL J2032.1+4049) does not appear in 3FGL [8].

4. Conclusion

The main differences of GAMMA-400 constructions from Fermi/LAT one are using the time-of-flight system with base of 50 cm and double layer structure of each plastic detectors provides more effective particles direction definition and backscplash rejection. Also two calorimeters in GAMMA-400 composed the total absorbtion spectrometer due to its total thickness ($\sim 25 X_0$ or $\sim 1.2 \lambda_0$ for vertical incident particles registration and $54 X_0$ or $2.5 \lambda_0$ for laterally incident ones (where λ_0 is nuclear interaction length)). It provides energy resolution 1-2% for $10 \text{ GeV} - 3.0 \times 10^3 \text{ GeV}$ events while the Fermi/LAT energy resolution does not reach such values because of its calorimeter thickness is only $\sim 10 X_0$. In the presented article, the event recognizing methods used in Fermi/LAT trigger system is considered in comparison with the ones applied in counting and triggers signals formation system of gamma-telescope GAMMA-400. Less than 3 % photons will be wrongly recognized as electrons or protons in double-layer A_{CTop} taking into account both temporal and amplitude trigger marker analysis methods during onboard processing in the counting and triggers signals formation system of GAMMA-400. The proton rejection factor will be $\sim 10^{-5}$. Moreover, the analysis shown that anticoincidence system of Fermi/LAT does not always work effectively (some protons are identified as γ -quanta, and on the other hand, some γ -quanta may be recognized as charged particles). Also some limitations occur during large amount of caveats methods for ground data processing. It leads to various biases, for example non confirmed announcement of $\sim 133 \text{ GeV}$ feature detection and lost sources in different Fermi catalogues (1FGL, 2FGL, 3FGL) – just well seen in 2FGL Cygnus X-3 (J2032.1+4049) does not appear in 3FGL. It allows to conclude sufficient biases in LAT characteristics obtained methods and event recognized algorithms. Respectively, continuation of measurements with use of other telescopes is necessary, and realization of GAMMA-400 will allow improving the results.

References

- [1]Ackermann M., Ajello M., Albert A. et al. (Fermi/LAT Collaboration) The Fermi large area telescope on orbit: event classification, instrument response functions, and calibration. *Astrophys. J. Suppl.* 2012;203(4):2-8.
- [2]Galper A.M., Adriani O., Aptekar R.L. et al. Status of the GAMMA-400 Project, *Adv. Space Res.*, 2013;51(2):297
- [3]Galper A.M., Adriani O., Aptekar R.L. et al. Characteristics of the GAMMA-400 Gamma-Ray Telescope for Searching for Dark Matter Signatures. *Bull. Russ. Acad. Sci. Phys.* 2013;77:1339-1342
- [4]Topchiev N.P., Galper A.M., Bonvicini V. et al. GAMMA-400 gamma-ray observatory. arXiv:1507.06246.
- [5]Arkhangelskaja I.V., Arkhangelsky A.I., Chasovikov E.N. et al. The counting and triggers signals formation system for gamma-telescope GAMMA-400. This Physics Procedia volume. 2015.
- [6]Swensen E., Ney S., Biehl F. et al. GLAST Tracker Mechanical Design. PDR Design Review Document. 2001; HTN-102070-0002.
- [7]Wren D.N. Detecting high-energy emission from gamma-ray bursts with EGRET and GLAST. *Dissertation.* 2005; LAT-TH-07960-01. University of Maryland (College Park, Md.).
- [8]Acero F., Ackermann M., Ajello M. et al. Fermi Large Area Telescope Third Source Catalog. *Astrophys. J. Suppl.* 2015;218(2, ID.23):1-41.
- [9]http://fermi.gsfc.nasa.gov/ssc/data/analysis/LAT_caveats_pass7.html
- [10]http://fermi.gsfc.nasa.gov/ssc/data/analysis/LAT_caveats_p7rep.html
- [11]Weniger C. A tentative gamma-ray line from Dark Matter annihilation at the Fermi Large Area Telescope. *JCAP.*1012;2012(8):007.
- [12]Park J.-Ch., Park S. Ch. Radiatively decaying scalar dark matter through U(1) mixings and the Fermi 130 GeV gamma-ray line. *Phys. Lett. B.* 2013;718(4-5):1401-1406.
- [13]Ackermann M., Ajello M., Albert A. et al. (Fermi/LAT Collaboration) Search for gamma-ray spectral lines with the Fermi Large Area telescope and dark matter implications *Phys. Rev. D.* 2013;88(8):082002.
- [14]Ackermann M., Ajello M., Albert A. et al. (Fermi/LAT Collaboration) Updated Search for Spectral Lines from Galactic Dark Matter Interactions with Pass 8 Data from the Fermi Large Area Telescope. *Phys. Rev. D.* 2015;91:122002.